

Single and Multi-Objective Real-Time Optimisation of an Industrial Injection Moulding Process via a Bayesian Adaptive Design of Experiment Approach

Mandana Kariminejad^{1,2,3,a}, David Tormey^{1,3,b}, Caitriona Ryan^{3,4,c}, Christopher O'Hara^{1,3,d},
Albert Weinert^{1,2,3,e}, Marion McAfee^{1,2,3,f,*}

¹Centre for Precision Engineering Material and Manufacturing Research (PEM Centre), Atlantic Technological University Sligo, Ash Lane, Sligo, F91 YW50, Ireland

²Centre for Mathematical Modelling and Intelligent Systems for Health and Environment (MISHE), Atlantic Technological University, Ash Lane, F91 YW50 Sligo, Ireland

³I-Form Advanced Manufacturing Research Centre, CSCB Building, O'Brien Centre for Science (East), University College Dublin, Belfield, Dublin 4, Ireland

⁴Trinity Centre for Ageing and Intellectual Disability, School of Nursing and Midwifery, Trinity College Dublin, the University of Dublin, Dublin 2, Ireland

^amandana.kariminejad@research.atu.ie, ^bdavid.tormey@atu.ie, ^cryanc86@tcd.ie, ^dchristopher.ohara@atu.ie,
^ealbert.weinert@research.atu.ie, ^fmarion.mcafee@atu.ie

* Correspondence: Marion McAfee

Abstract

Minimising cycle time without inducing quality defects is a major challenge in the injection moulding (IM). Design of Experiment methods (DoE) have been widely studied for optimisation of the IM, however existing methods have limitations, including the need for a large number of experiments and a pre-determined search space. Bayesian adaptive design of experiment (ADoE) is an iterative process where the results of the previous experiments are used to make an informed selection for the next design. In this study, for the first time, an experimental ADoE approach, based on Bayesian optimisation, was developed in injection moulding using process and sensor data to optimise the quality and cycle time in real-time. A novel approach for the real-time characterisation of post-production shrinkage was introduced, utilising in-mould sensor data on temperature differential during part cooling. This characterisation approach was verified by post-production metrology results.

A single and multi-objective optimisation of the cycle time and temperature differential (ΔT) in an injection moulded component is proposed. The multi-objective optimisation techniques, composite desirability function and Nondominated Sorting Genetic Algorithm (NSGA-II) using Response Surface Methodology (RSM) model, are compared with the real-time novel ADoE approach. ADoE achieved almost a 50% reduction in the number of experiments required for the single optimisation of ΔT , and an almost 30% decrease for the optimisation of ΔT and cycle time together compared to composite desirability function and NSGA-II. Also, the optimal settings identified by ADoE for multiobjective optimisation were similar to the selected Pareto optimal solution found by the NSGA-II.

Keywords: Injection moulding, Gaussian Process, Bayesian Adaptive Design of Experiments, Multi-objective optimisation, Nondominated Sorting Genetic Algorithm

1. Introduction

Injection moulding (IM) is one of the leading manufacturing processes for the mass production of complex-shaped plastic components that require high precision. The quality and efficiency of the process depend strongly on finding the optimum process settings, monitoring the process inline, and adapting the settings as needed to prevent defects in the component (Zhao et al., 2020). Non-uniform temperature distribution on the cooling of the part is one of the main causes of part defects, leading to residual stresses, shrinkage, and warpage. For precision components, ensuring dimensional stability is crucial, requiring the elimination of shrinkage and warpage to meet the dimensional tolerances and prevent potential failures. Locally heated regions in the component, known as hotspot locations, must be identified and minimised to prevent residual stresses, which lead to the gradual manifestation of shrinkage and warpage in the days/weeks following production.

Besides component quality, another critical parameter that directly affects the efficiency and cost of the process is cycle time. The cycle time of the IM process is the total time required to complete all the stages including mould closing, filling, packing, cooling, mould opening and ejection. Achieving the shortest possible cycle time while producing a product without defects is challenging. Several efforts have been made to minimise hotspots by redesigning cooling channels and runner systems and modifying the machine tools (Luh et al., 2019; Oh et al., 2022). However, the complete elimination of hotspots through the tool design is rarely possible for complex parts, and it is important to find the process settings required for optimum temperature distribution, part quality and cycle time.

Various research works have previously examined the problem of finding the optimum process settings to minimise defects or cycle time in industrial processes using different design of experiment (DoE) approaches. Classic design of experiment (DoE) approaches are commonly used to model the relationship between the process variables and desired responses. One of the popular DoE approaches used in industry is response surface methodology (RSM). One of the main categories of RSM is central composite design (CCD). For multi-objective optimisation, a classic DoE method needs to be combined with other optimisation approaches such as desirability function, Genetic Algorithm (GA), Artificial Neural Network, or Particle Swarm Optimisation (PSO), etc.

Mukras et al. applied CCD along with other optimisation approaches to find the relationship between part quality factors and seven process parameters (Mukras, 2020; Mukras et al., 2019). In (Mukras, 2020), the surface plot data from CCD was used to formulate an optimisation problem for finding the minimum cycle time with product shrinkage and warpage constraints. They solved the optimisation problem using nonlinear constrained optimisation and validated their model via experiment. In (Mukras et al., 2019), CCD was applied along with a GA to optimise a multi-objective problem that could achieve the minimum component warpage and shrinkage. They validated their approach via experiment, where a 7% error was found between the predicted optimal results and the actual experimental results. Zhijun et al. (Zhijun et al., 2019) established a multiobjective optimisation approach using CCD and GA to optimise warpage and sink marks in the seat belt cover plate of a car. The comparison of the theoretical and experimental values for warpage and sink marks indicated 0.2% and 7.95% error respectively.

Sudsawat et al. (Sudsawat & Sriseubsai, 2018) applied CCD combined with the firefly algorithm (Kumar & Kumar, 2021) to find the optimum process settings for minimising the warpage of an injection moulded component. Their method found suitable process parameters that reduced the component warpage by almost 23% compared to the recommended settings calculated by Moldex3D, (a commercial simulation software package for injection moulding), and empirical tests. Toh and Hassan (Toh & Hassan, 2021) applied CCD to find the optimum mould temperature and packing pressure required to minimise the warpage and flash in a multi-cavity injection moulding process. The overlaid contour plots for the eight cavities and both responses led to finding the feasible region to minimise the response. The results were validated through physical experiments. A detailed review of recent studies applying classic DoEs with various optimisation techniques in IM since 2018 is listed in Table 1.

In these classic design of experiment approaches, the sampling and experiment patterns are deterministic and cannot change or adapt to the features that appear during the experiment. Typically, a large number of experiments are required for effective optimisation, and this may have to be repeated multiple times, for example on changing material batch or supplier. Also, employing robust and strong global optimisation techniques like firefly algorithm, MOPSO, MOGA, and NSGA-II alongside classic DoEs across diverse applications (Liu et al., 2022; Pareek et al., 2023; Sun et al., 2022; Yang et al., 2023), often enhances model performance and optimisation effectiveness. However, these methods unlike ADoE, often lack in efficiently sampling the experimental space and enabling inline optimisation and mainly rely on traditional DoE for data generation.

Adaptive design of experiment (ADoE), on the other hand, is an iterative process where the results of the previous experiment are used to make an informed selection for the next design. The adaptive approach has several advantages over classic DoEs like RSM. Firstly, it is tailored to the design process (incorporating prior knowledge). Secondly, the search and optimisation processes are rapid, and the number of experiments is reduced due to the exploitation of prior knowledge to reduce the complexity and accelerate the process. Thirdly, adaptive methods can search in a high-dimensional space, while classic DoEs have a limited search space. Finally, ADoE can be used in multi-objective optimisation problems (Greenhill et al., 2020). ADoE has been enabled through a combination of machine-learning approaches applied to the experimental design. Bayesian optimisation (BO) is a useful tool for ADoE using adaptive sampling to find a global optimum for a response. It can be applied even when the objective function is unknown or complex, the evaluation of the objective function is expensive, and when the gradient information is unavailable (Anand et al., 2010; Shahriari et al., 2016).

Table 1- Previous studies on the optimisation of IM using classic DOEs since 2018

DoE method	Objective(s)	Optimisation approach	Reference
Orthogonal testing	Warpage, Shrinkage	NSGA-II	(Fang et al., 2022)
Latin Hypercube Design	Warpage, Shrinkage	NSGA-II	(Lu & Huang, 2020)
Box-Behnken	Max shrinkage, Volume shrinkage, addendum & circle diameters shrinkage	NSGA-II	(Wu et al., 2022)
RSM	Warpage, residual stresses	PSO (simulation)	(Nguyen et al., 2022)
CCD	warpage	Firefly algorithm	(Sudsawat & Sriseubsai, 2018)
CCD	Cycle time	Nonlinear constrained optimisation	(Mukras, 2020)
CCD	Warpage, shrinkage	GA	(Mukras et al., 2019)
CCD	Warpage, flash	Overlaid contour plots	(Toh & Hassan, 2021)
CCD	Warpage, sink marks	GA	(Zhijun et al., 2019)
Taguchi	Warpage, shrinkage, residual stresses	Nondominated Sorting Genetic Algorithm II (NSGA-II)	(Li et al., 2019)
Taguchi	Surface roughness, shrinkage	Composite desirability function	(Usman Jan et al., 2020)
Taguchi	Warpage, clamp force, weld line	ANN- MOGA	(Feng et al., 2020)
Taguchi	Cycle time, warpage	Composite desirability function	(Singh et al., 2018)
Taguchi	Shrinkage, warpage, short shot	Fuzzy decision-making process	(Moayyedean & Mamedov, 2019)
Taguchi	Mechanical properties, shrinkage	multi-criteria decision making (MCDM) & NSGA-II	(Öktem & Shinde, 2021)

ADoE and BO approaches have emerged from initial application in medical science for dose-finding studies (McGree et al., 2012), to recent investigations in industrial applications, such as metal processing to optimise alloy composition and heat treatment (Vahid et al., 2018; D. Xue et al., 2016), waste treatment process (Cho et al., 2023), and additive manufacturing to optimise metamaterial composite, lattice structure design and process parameters (Kim et al., 2022; Mondal et al., 2020; Sharpe et al., 2018; T. Xue et al., 2020). However, to date, there are few practical studies of ADoE in manufacturing and none in relation to polymer processing, despite recent efforts in multiobjective optimisation of such processes using traditional DoE methods with modern optimisation algorithms as outlined above.

There have been a few attempts using adaptive DoE for single response optimisation of the injection moulding process through simulation models. These studies (Gao & Wang, 2009; Xia et al., 2011; Zhou & Turng, 2007) devised kriging and GP surrogate models to find the relationship between process parameters and warpage through simulation. The final optimum process parameters found with these approaches showed a good convergence with the experimental results of warpage. Recently, Jung et al. applied Bayesian optimisation for multi-objective optimisation of warpage and cycle time (Jung et al., 2022), also using Moldflow simulation. They compared the Bayesian optimisation method to a constrained generative inverse design network (GIDN), which uses backpropagation to find the gradient of an objective function. Simulation software was used for applying both methods. The results showed the efficiency of both approaches in multi-objective optimisation, while the Bayesian framework had a better performance in adapting to the variations in responses with a smaller dataset required.

The above studies employed data from simulation software to develop the surrogate model and optimise the part quality. However, basing the process optimisation on simulation software such as Moldflow and Moldex has several drawbacks. Each simulation is extremely time intensive (several hours), purchasing the software is costly, and the calculations are not precise since the parameters of the material are often not well defined or may even change from batch to batch. Hence an efficient experimental method of process optimisation is required to overcome these shortcomings.

The challenge in applying adaptive approaches experimentally is that the product quality in terms of dimensional stability is not known until metrology measurements have been obtained, usually a week or more post-production. Hence, in order to explore the potential benefits of an ADoE approach, a rapid indicator of dimensional stability is required. The part temperature distribution is a good indicator of the product quality since a uniform temperature profile eliminates thermally-induced residual stresses and hence shrinkage or warpage. This study proposes a real-time indicator of temperature profile for part quality evaluation in terms of the temperature differential between a known hotspot location in the component and a location with average temperature using two in-mould thermocouples.

This paper, for the first time, investigates the practical effectiveness of the Bayesian Optimisation ADoE compared to a classic DoE approach, in a practical injection moulding process, based on in-line measurements. The objective is to find the optimum process settings that minimise both the cycle time and the temperature

differential (ΔT) between a part hotspot and an average temperature point, which has been validated in the study to correlate to post-production shrinkage. The main novelties of this study are (1) the introduction of a real-time monitoring method demonstrated to be a suitable proxy for post-production shrinkage measurements, and (2) validation of an intelligent adaptive design of experiment (ADoE) method for multi-objective optimisation in an injection moulding process using experimental data. This research shows the suitability of the in-line method for predicting the dimensional stability of the part and the superior performance of ADoE approach in finding the optimum process settings with significantly fewer experiments than CCD.

The remainder of the paper is organised as follows. The theory section outlines the methods used in the study, including Bayesian ADoE, CCD, optimisation by desirability function and NSGA-II. Section 3 details the methodology, including experimental set-up, design and data collection, and details on the optimisation methods applied.. The corresponding results and discussion of the experimental studies are defined in section 4, followed by a conclusion with suggested further research.

2. Theory

2.1 Bayesian ADoE

Bayesian optimisation (BO) consists of two main components: a statistical and probabilistic surrogate model to estimate the black-box objective function, and an acquisition function to decide on the next sampling point (Frazier, 2018).

A Gaussian process (GP) regression is typically considered the best choice for creating the surrogate model. It can estimate the values of the black-box function $f(x)$ at the point x , by providing a posterior probability distribution. $f(x)$ is gaussian if any vector of $x = [x_1, x_2, \dots, x_n]^T$ such that $x_i \in X$ (input space), the vector of output $f(x) = [f(x_1), f(x_2), \dots, f(x_n)]^T$ is gaussian distributed with mean $[m(x_1), m(x_2), \dots, m(x_n)]^T$.

The GP considers the prior distribution to be normal and is specified by a mean vector $\mu(x)$ and a covariance matrix $k(x, x')$ between $f(x)$ and $f(x')$ where x and x' are a pair of observations:

$$f(x) \sim \text{Gaussian}(\mu(x), k(x, x')) \quad (1)$$

The covariance matrix, also called a kernel, captures the smoothness of the process. If x and x' are close to each other, then their associated values for the output ($f(x)$ and $f(x')$) will also be close, and the closeness can be estimated by the distance between these two points. One commonly used kernel is the Matern kernel, defined in equation 2. $k(v)$ is a modified Bessel function, Γ is the gamma function, ν (known as a smoothness parameter) and α_0 are the hyperparameters.

$$k(x, x') = \alpha_0 \frac{2^{1-\nu}}{\Gamma(\nu)} (\sqrt{2\nu} \|x - x'\|)^{\nu} K(\nu) (\sqrt{2\nu} \|x - x'\|) \quad (2)$$

If the ν is a half-integer (1/2, 3/2, and 5/2), the kernel will be a product of an exponential and a polynomial function, as written in equation 3.

$$\begin{aligned} k(x, x')_{\nu=1/2} &= \alpha_0 \exp(-\|x - x'\|) \\ k(x, x')_{\nu=3/2} &= \alpha_0 \exp(-\sqrt{3}\|x - x'\|) (1 + \sqrt{3}\|x - x'\|) \\ k(x, x')_{\nu=5/2} &= \alpha_0 \exp(-\sqrt{5}\|x - x'\|) (1 + \sqrt{5}\|x - x'\| + \frac{\sqrt{5}}{3} \|x - x'\|^2) \end{aligned} \quad (3)$$

In a physical experiment, observations can generally be considered subject to normally distributed noise $\varepsilon \sim N(0, \sigma^2)$ and the objective function at point x can be written as:

$$y = f(x) + \varepsilon \quad (4)$$

For the prediction of the objective function at the new point x , we consider $D_{1:n} = \{(x_i, y_i)\}$ and the result is a normal distribution with mean $\mu(x)$ and variance $\sigma_n^2(x)$, the objective function can be calculated based on equation 5.

$$\begin{aligned} p(f(x) | D_{1:n}, x) &= N(\mu_n(x), \sigma_n^2(x)) \\ m_n(x) &= m(x) + k(x, x_{1:n}) [k(x_{1:n}, x_{1:n}) + \sigma_{noise}^2 I]^{-1} (y_{1:n} - \mu(x_{1:n})) \\ \sigma_n^2(x) &= k(x, x) - k(x, x_{1:n}) [k(x_{1:n}, x_{1:n}) + \sigma_{noise}^2 I]^{-1} k(x_{1:n}, x) \end{aligned} \quad (5)$$

$$k(x, x_{1:n}) = [k(x, x_1), k(x, x_2), \dots, k(x, x_n)], \quad k(x_{1:n}, x_{1:n}) = \begin{bmatrix} k(x_1, x_1) & \dots & k(x_1, x_n) \\ \vdots & \ddots & \vdots \\ k(x_n, x_1) & \dots & k(x_n, x_n) \end{bmatrix}$$

The second element of BO is an acquisition function (AF) which can be calculated from the mean and variance of the GP model, meaning it is rapid and inexpensive to compute. The acquisition function decides which area of the input domain maximises exploitation (where the objective mean is high) and exploration (where the uncertainty is high) for the next evaluation of the black-box function $f(x)$. For example, the AF value is small in the areas where $f(x)$ is suboptimal or has already been searched. The desired next experimental setting is where the AF is maximum.

There are various types of AFs, and one commonly used choice is Expected Improvement (EI), proposed originally by (Moćkus, 1975).. The EI can be calculated as equation 6, where $f(x^*)$ is the current maximum, Φ is the cumulative distribution function (CFD), and ϕ is the probability distribution function (PDF) of the normal distribution to balance between exploration and exploitation. For maximising the EI based on this equation, first $m_n(x) > f(x^*)$ and second by increasing the variance $\sigma_n(x)$.

$$EI(x) = (m_n(x) - f(x^*))\phi\left(\frac{\mu_n(x) - f(x^*)}{\sigma_n(x)}\right) + \sigma_n(x)\Phi\left(\frac{\mu_n(x) - f(x^*)}{\sigma_n(x)}\right) \quad (6)$$

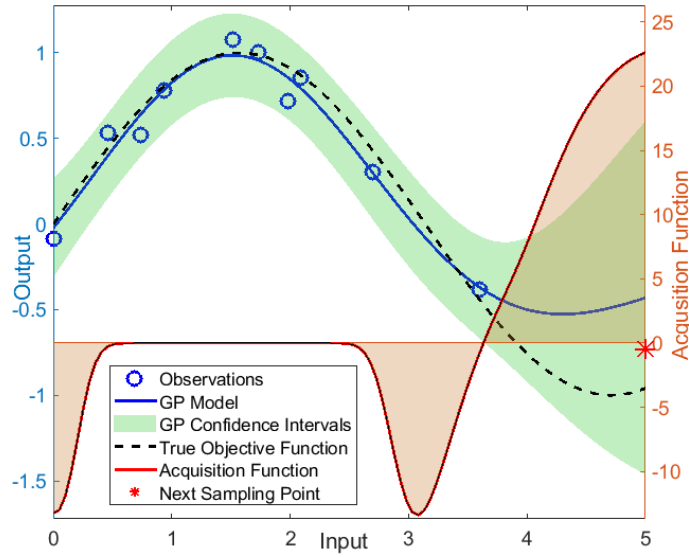


Fig. 1. Bayesian Optimisation

Fig. 1 illustrates the BO process. A Gaussian Process surrogate model is fitted to some observations with the uncertainty (confidence intervals) shown by the green area. The red plot represents the fitted acquisition function based on the Gaussian Process model and illustrates that the AF is high in previously unsampled regions where the mean of the AF is also predicted to be high. The next sample point is chosen as the point where the AF is maximum (indicated red star in the graph). For further in-depth reading on the theory of Bayesian optimisation and adaptive design of experiments, the reader is referred to the following references (Greenhill et al., 2020; Hoffer et al., 2023; Imani & Ghoreishi, 2020; Pandita et al., 2021).

2.2 Optimisation using the desirability function

The desirability function, or multiple response optimisation, was developed by Derringer and Suich (Derringer & Suich, 1980) and is a technique that transforms a multi-objective optimisation problem into a scale-free value known as desirability. This method integrates these individual objectives into a single optimisation problem, rather than solving them separately.

The optimisation consists of two main steps. First, the value of each response is assigned to a dimensionless desirability d_i that $0 < d_i < 1$. For values of d_i near 0, the response is undesirable; on the contrary, the response for values of d_i close to 1 is desirable. Secondly, each of the desirability values are combined into an overall desirability function, called D , that is calculated using equation 9, where n is the number of responses and (y_i) is the desired response. A weight (w_i) can also be assigned to each response based on its effect on the final objective to adjust the desirability function as in equation 9.

$$D = \left(\prod_{i=1}^n d_i(y_i) \right)^{1/n} = [d_1(y_1) \times d_2(y_2) \times \dots \times d_n(y_n)]^{1/n} \quad (8)$$

$$D = [d_1(y_1)^{w_1} \times d_2(y_2)^{w_2} \times \dots \times d_n(y_n)^{w_n}]^{1/n} \quad (9)$$

In an optimisation problem, the desired response can be minimised, maximised, or set as a target value. A single response optimisation indicates how the input variables affect the desirability of the related response. In this research, the desired responses are cycle time and the temperature differential between a hotspot and a point of average temperature. The goal is to minimise these two values. The desirability function for minimisation with a weight equal to 1 (since both responses were considered to have the same importance on the quality of the component) for each of the responses is described by equation 10, where y_{min} and y_{max} are the minimum and maximum acceptable values for the response y_i (Lee et al., 2018). The multi-objective optimisation by desirability function in this paper was carried out using a response optimiser in statistical software Minitab 20.

$$d_i(y_i) = \begin{cases} 1 & \text{if } y_i \leq y_{min} \\ \frac{y_{min} - y_i}{y_{max} - y_{min}} & \text{if } y_{min} \leq y_i \leq y_{max} \\ 0 & \text{if } y_i \geq y_{max} \end{cases} \quad (10)$$

2.3 Non-dominated Sorting Genetic Algorithm (NSGA-II)

NSGA-II is an evolutionary algorithm developed to overcome the shortcoming of classical multiobjective optimisation approaches which convert the optimisation problem into a single objective optimisation. It incorporates mechanisms to include elitism and preserve diversity. It has two further stages compared to GA: non-dominated sorting and crowding distance ranking

In non-dominated ranking individuals (chromosomes) are sorted into Pareto fronts based on their dominance. In dominance relation, solution p dominates solution q (denoted as $p \leq q$) if for all objectives solution p is at least as good as solution q and strictly better in at least one objective. In other words, a solution is Pareto optimal if it is not dominated by any other solution in the objective space. A set of Pareto optimal solutions, also called the Pareto front, represents the trade-off between the conflicting objectives. Crowding distance estimates the density of the solutions around a specific solution in the objective space. It maintains diversity in the population and guides the search towards the Pareto front (Deb, 2011; Deb et al., 2002). Fig. 3 represents the principle of the NSGA-II algorithm.

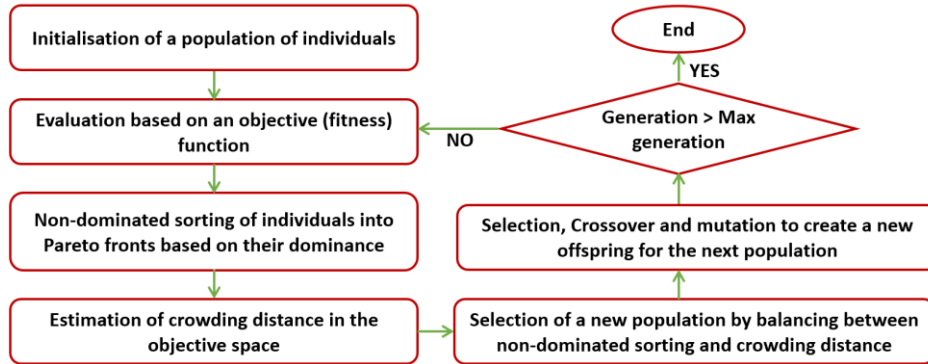


Fig.3. Flowchart of NSGA-II optimisation algorithm

3. Methodology

3.1 Equipment and Sensorisation

The isometric view and dimensions of the injection moulded part, referred to as the Clip, are shown in Fig. 4(a). The material of the component is POM (Polyoxymethylene), and the Clip is currently being manufactured by an industrial partner with issues such as excessive cycle time and part shrinkage. In our previous research (Kariminejad et al., 2022), the temperature distribution and hotspot regions were identified within the part through Moldflow simulation software as shown in Fig. 4 (b).

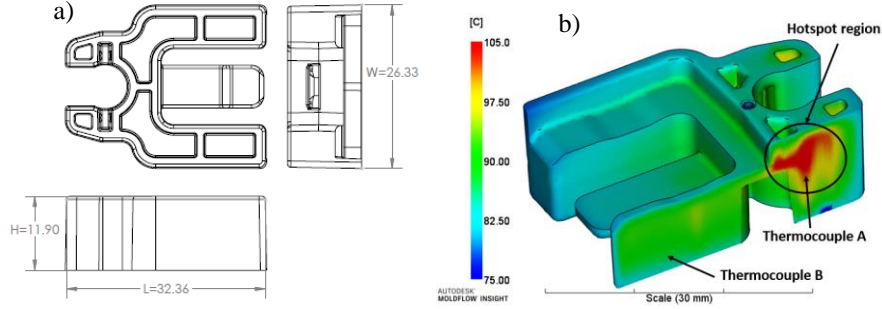


Fig. 4. a) Clip main dimensions in millimetres. b) temperature distribution in part by simulation (Kariminejad et al., 2022)

Sensors are required to measure the temperature distribution during the experiments and extract accurate real-time data that can be used for optimisation. For direct in-mould temperature measurements where the sensor is in contact with the polymer melt, Kistler high-temperature thermocouples (type 6193B0,4) were chosen. The key selection criteria include the sensor temperature durability of up to 450°C and the small size (diameter of 1mm) needed to fit into the cavity.

Informed by the Moldflow simulation results, sensor locations were identified and two direct Kistler thermocouples were placed in the mould insert, one to take measurements of the identified hotspot point (Thermocouple A) and another to measure a point with average temperature (Thermocouple B) based on the simulation results in Fig. 4(b). Fig. 5 shows the 3D view, the manufactured moving half of the mould inserts with the embedded thermocouples and the manufactured product (Clip).

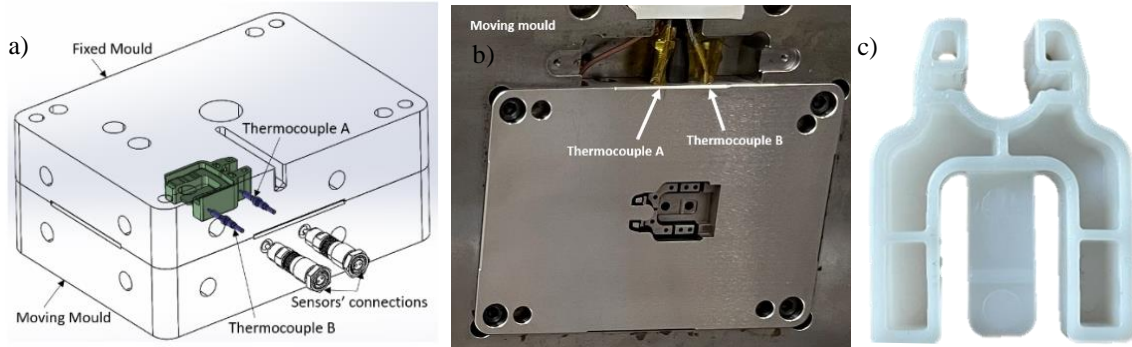


Fig. 5. a) Isometric view of the sensors in the mould tools. b) Manufactured mould tools and the moulded clip

3.2 Screening of the parameters and CCD implementation

This study aimed to optimise two responses. The first response of interest is the temperature differential (ΔT). In section 4.1, it is validated that ΔT correlates with shrinkage and has been chosen as the quality index to update the model in real-time. ΔT can be measured by calculation of the difference between thermocouple readings from thermocouple A (the hotspot location) and thermocouple B (the average temperature) in Fig. 3 and 4 and it can be written as follows:

$$\Delta T (^{\circ}\text{C}) = T_{TCA} - T_{TCB} \quad (11)$$

The second response is cycle time, which can be recorded from the control panel of the injection moulding machine for each cycle. The only process variables that influence the cycle time are cooling and packing (holding) time which can be defined in the machine settings. In comparison, there are many process parameters that will affect the temperature differential. If all of the input variables are considered, the number of experiments will be very high. Hence screening is essential to evaluate the main variables and their interaction effects on the desired outputs. Eight process parameters were first chosen to screen the main design variables, and then the insignificant parameters were removed from consideration in the implementation of ADoE and CCD. Analysis of Variance (ANOVA) was applied to identify the main variables and interactions.

The eight parameters were: mould temperature, melt temperature, holding time, holding pressure, shot size, switch-over position, injection speed, and cooling time. A two-level fractional factorial design was used for the initial screening analysis. The variables with their upper and lower limits are shown in Table 2.

Table2. Selected process parameters and levels for screening

Level	Holding time (s)	Mould temperature (°C)	Holding pressure (bar)	Shot size (mm)	Switch over position (mm)	Injection velocity (mm/s)	Barrel temperature (°C)	Cooling time (s)
Low	3	40	200	6	5	20	210	10
High	6	90	400	12	10	40	230	30

The number of experiments for the fractional factorial method with a 1/16 fraction and eight two-level variables was 16. Each experiment design was repeated ten times (ten manufactured parts) to ensure stability, preserve data for part quality evaluation via metrology and to capture natural process variation during the process. To calculate the temperature differential (ΔT) in each run, the average of each temperature sensor reading was calculated during the ten cycles and then the difference between the two averages was determined as per equation 12.

The variables having a significant effect on ΔT were selected from all eight variables to use in the ADoE and CCD experimental designs based on the screening results. A full central composite design was then applied using the process variables obtained in the screening section with the aim of having an accurate quadratic model and investigating the interaction between the variables. The design optimiser was used to find the optimum settings for the ΔT and cycle time by using the desirability function in equation 11. The related results of screening of the parameters and CCD is detailed in section 4.2.

3.3 ADoE

The adaptive DoE required an initial sample data set, which is used to predict the next experimental designs. For the initial dataset, twelve experiments were randomly chosen from the CCD.

The software package used in this paper for BO is ‘mlrMBO’ (Bischl et al., 2017). It has the advantages of providing a good range of acquisition functions and it is suitable for multi-objective problems. Gaussian process model was chosen as the surrogate model, and the acquisition function was EI (expected improvement).

The data from the initial twelve experiments was used as prior data for the Bayesian optimisation algorithm to predict the design of the next two new experiments. Since the responses were collected inline during the process optimisation, the next two experiment settings were generated in the ADoE approach to save time in computing the next settings between every experiment. These two experimental designs were conducted for ten shots in the injection moulding machine to ensure the stability of the process and provide data for metrology.

The ΔT was measured using the sensor data (equation 11), and the cycle time was also recorded. Then these two new designs were added to the initial dataset and fed into the ADoE to predict the next two experiment designs. This was repeated until it was observed that the recommended process settings had converged. The criterion for the stopping point was stability or convergence of the input parameters for single objective optimisation. The stopping point for the multiobjective optimisation was defined by reaching the minimum thresholds set for the objectives. The thresholds were 7°C on ΔT and 33s on cycle time. If any solution found during the BO meets or exceeds the threshold for the objectives, the BO can be considered successful. Fig. 6 compares the optimisation process using the Bayesian adaptive design of experiment with desirability function and NSGA-II.

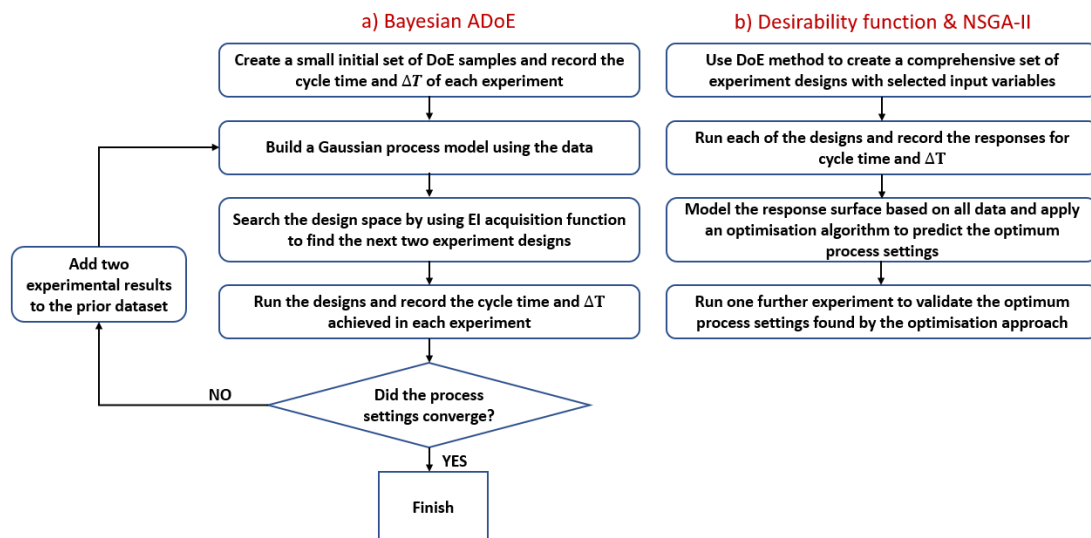


Fig. 6. a) Bayesian ADoE and b) Desirability function & NSGA-II optimisation flowcharts

3.4 Optimisation with NSGA-II and desirability function

For modelling the relationship between the input parameters and each of the objectives (ΔT and cycle time) different models were investigated using the CCD dataset; Artificial Neural Network (ANN) and Gaussian process (GP) modelling with fivefold cross-validation and the quadratic RSM model obtained from CCD. The ANN model utilised a feedforward architecture featuring ten neurons and Rectified Linear Unit (ReLU) activation function. The GP model employed a Gaussian kernel, and the hyperparameters, including the variance of the Gaussian process and the length scale parameter, were optimised through maximum likelihood estimation (ML).

Table 3 summarises the RMSE of each method for each of the outputs. From the Table RSM model outperformed the other two methods since it has a lower RMSE for both cycle time and ΔT .

Table 3- Comparing ANN, GP, and RSM models

Model	Average RMSE ΔT (°C)	Average RMSE cycle time (s)
ANN	0.68	2.36
GP	0.32	1.02
RSM	0.21	0.95

After finding a suitable model for each of the objectives, NSGA-II was applied to search for the optimal outputs based on the flowchart in Fig. 3. The algorithm was initiated with a population size and maximum iteration of 100 and a crossover probability of 0.8. The RSM model was also integrated with desirability function to find the optimal process settings, first with ΔT as the response variable and then for two response variables: ΔT and cycle time.

3.5 Metrology

After conducting the experiments, an OGP Smartscope CNC 500 dimensional multi-sensor coordinate measuring machine (CMM) with a resolution of $0.5\mu\text{m}$ was used for evaluating dimensional measurements. The physical measurements were taken at least two weeks after the production of the components to ensure no further variation in the dimensions on the relaxation of residual stresses. The CMM measurements were used to correlate the process settings with maximum, minimum, and average temperature differential (ΔT) and verify the relationship between ΔT and shrinkage.

Three main or critical dimensions shown in Fig. 2 (L, H, and W) were chosen for dimensional evaluation with a tolerance of $\pm 0.2\text{mm}$, specified by the industrial partner. Fig. 7 illustrates the CMM machine measuring ten clip components on a designed fixture. Based on this validation, the component with the maximum ΔT and the minimum ΔT should have the maximum and minimum shrinkage, respectively.



Fig. 7. OGP Smartscope CNC 500 measuring the main dimensions of Clip.

4. Results & Discussion

4.1 Metrology

Parts produced under a range of different process settings were chosen for metrology investigation for the evaluation of the correlation between ΔT and shrinkage post-production. The selected experiments are listed in Table 4, and ΔT is presented in descending order for clarity.

In Table 5, the tolerances are defined as percentages by considering 100% equal to the specified product tolerance of $\pm 0.2\text{mm}$. Each main dimension with a value less than 100% is in an acceptable range, meaning post-production shrinkage has not significantly occurred in the component. For each experiment, the tolerances of ten components were measured and the average value was calculated and noted in Table 4 with their corresponding standard deviations. For better visualisation, Fig. 8 summarises Table 4 into a bar graph and illustrates the tolerance deviation from the baseline of 100% ($\pm 0.2\text{mm}$) for each of the dimensions in each experiment. Based on Table 4 and Fig. 8, the reduction in ΔT led to a decrease in tolerance variation of each critical dimension, and

for the optimum process settings found by ADoE, no shrinkage was observed in any dimension. Hence, this correlation validates that ΔT can be considered as the shrinkage index to be used in real-time in the ADoE approach. Incorporating shrinkage as the objective necessitates waiting for post-production shrinkage, a process that takes up to several weeks as the residual stresses gradually relax over time. In contrast, optimising based on ΔT enables inline and rapid adjustments.

Table 4. Metrology results, presented in descending order of ΔT recorded in-process

No.	Run type	Run number	Actual ΔT (°C)	ΔT - type	Cycle time (s)	Tolerance deviation (Standard deviation)		
						L (%)	H (%)	w (%)
1	ADoE-Multiobjective	4	10.19	Maximum	29.8	150.4 (22.8)	50.75 (20.12)	152.25 (7.8)
2	ADoE-multiobjective	9	7.77	Average	28.8	137.8 (4.4)	47.75 (21.47)	142.75 (4.6)
3	CCD	23	7.63	Average	33.3	77 (5.04)	35.3 (25)	122.75 (9.4)
4	Multiobjective desirability function optimum setting	-	7.42	Average	28.8	57.4 (6.8)	48.8 (36.5)	90.8 (3.6)
5	ADoE-multiobjective optimum setting	10	6.51	Minimum	32.9	52 (3.8)	42 (16.15)	85.6 (5.44)
6	ADoE & desirability function-single-optimum setting	4	5.54	Minimum	44.8	46.6 (1.03)	24.75 (15.19)	78.5 (4.24)

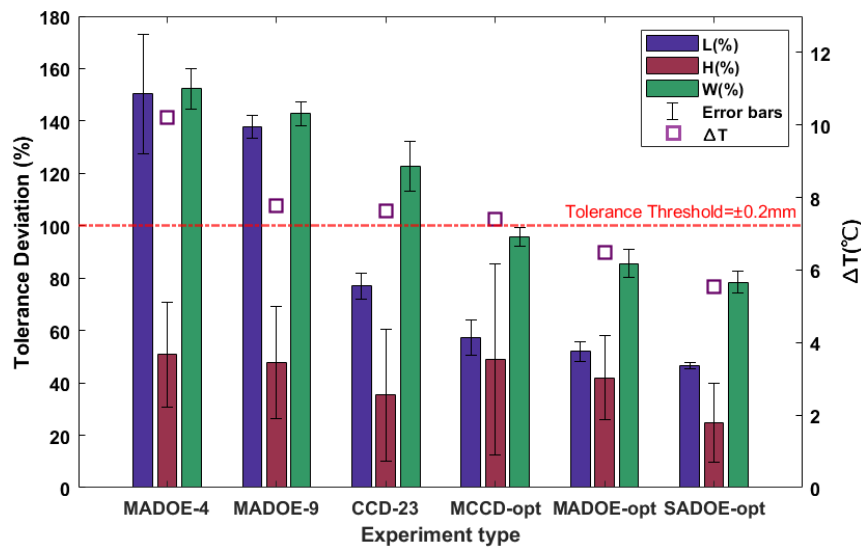


Fig. 8. Bar graphs of the tolerance deviation of the main dimensions in Clip. MADOE refers to multiobjective ADOE and for the examination of metrology in MADOE experiment numbers 4, 9 and the optimum setting found by ADOE were selected. MCCD-opt refers to multiobjective optimisation using CCD and desirability function. SADOE means the single objective optimisation of ΔT using ADOE.

4.2 Screening and CCD step

The effect of eight input parameters on the ΔT was investigated using fractional factorial design in Minitab 20. A 95% confidence bound was selected, such that any variables with a p-value lower than 0.05 were deemed significant.

Fig. 9 (a) and (b) show the normal plots and Pareto chart of the effects from analysis of variance (ANOVA). Based on Fig. 9, the mould temperature, cooling time, holding time, barrel (melt) temperature, the interaction between cooling time and holding time, and the switch-over position affected the ΔT . The parameters identified in this study align with the findings of previous research on effective process parameters on warpage in IM process. For example, previous studies on plastic product warpage and shrinkage (Roslan et al., 2021; Sudsawat & Sriseubsai, 2018; Wen et al., 2014; Zhang & Jiang, 2007) identified melt temperature, mould temperature, packing time, cooling time, and switch-over position as the most influential process parameters on shrinkage and warpage. It is essential to emphasise that process parameter screening for cycle time was not conducted since the only influential process parameters on cycle time are packing time and cooling time, both were considered as process inputs in the optimisation problem.

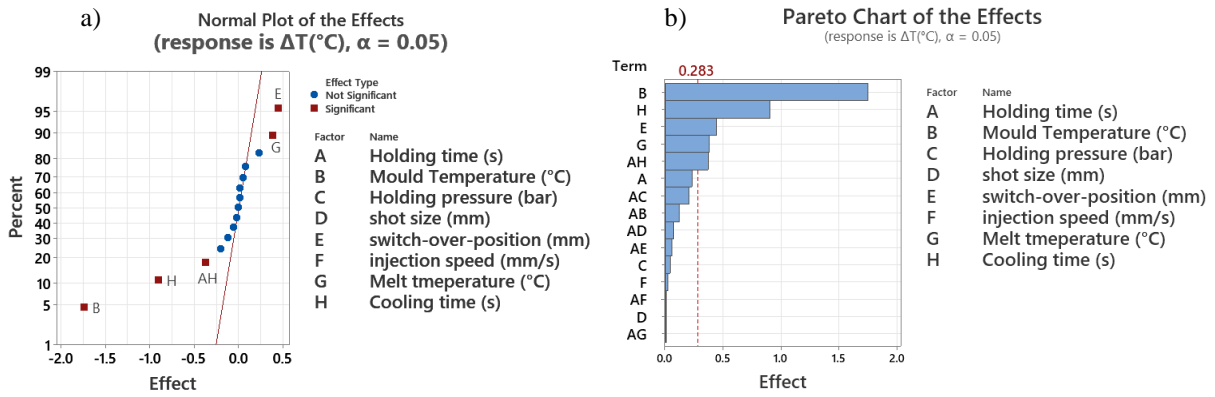


Fig. 9. a) Normal plots and b) Pareto chart of ANOVA for screening

Based on screening results, four variables were selected for the optimisation to use in CCD and ADoE. These were: mould temperature, cooling time, holding time, and barrel (melt) temperature, as detailed with their respective levels in Table 5. The switch-over position depends on the shot size and leftover melt cushion; this is challenging to modify during the injection moulding machine cycles. Although it was identified as an influential design variable in ANOVA, it was removed from the main process parameters for this reason. The selected CCD method in this study is circumscribed (CCC), and the α value is equal to 2.

Table 5. Selected process parameters and levels for CCD

Parameters	Level				
	$-\alpha$	-1	0	+1	$+\alpha$
Mould Temperature (°C)	55	65	75	85	95
Cooling time (s)	15	20	25	30	35
Holding time (s)	1.5	3	4.5	6	7.5
Barrel Temperature (°C)	195	205	215	225	235

The number of experiments for a full CCD design, using four input variables ($f = 4$) and six replications at the centre point ($r = 6$), is 31. The experiments were designed using Minitab 20 software. Table 6 shows the experimental designs for the CCD and the assigned values for the cycle time and average ΔT for each experiment.

Table 6. CCD design and results for the average ΔT and cycle time

Experiment No	Mould Temperature (°C)	Cooling time (s)	Holding time (s)	Barrel Temperature (°C)	Avg ΔT (°C)	Cycle time (s)
1	65	30	3	205	7.6	40.3
2	65	20	6	205	8.84	33.3
3	75	25	4.5	215	8.12	36.8
4	75	25	4.5	215	8.22	36.8
5	65	20	3	205	9.8	30.3
6	75	25	4.5	215	8.1	36.8
7	65	20	6	225	9.46	33.3
8	85	30	6	225	6.82	43.3
9	75	25	4.5	215	8.17	36.8
10	75	25	4.5	215	8.17	36.8
11	65	30	3	225	8.1	40.3
12	75	35	4.5	215	6.78	46.8
13	95	25	4.5	215	7.1	36.8
14	85	30	6	205	6.5	43.3
15	75	25	1.5	215	8.23	33.8
16	55	25	4.5	215	8.74	36.8
17	75	15	4.5	215	9.62	26.8
18	75	25	4.5	235	8.4	36.8
19	75	25	7.5	215	7.63	39.8
20	85	30	3	205	6.66	40.3
21	75	25	4.5	215	8.1	36.8
22	85	20	6	225	8.40	33.3
23	85	20	6	205	7.63	33.3

24	65	30	6	205	6.97	43.3
25	85	20	3	225	8.37	30.3
26	65	20	3	225	9.34	30.3
27	65	30	6	225	8.27	43.3
28	85	30	3	225	6.94	40.3
29	85	20	3	205	8.03	30.3
30	75	25	4.5	195	7.7	36.8
31	75	25	4.5	215	7.94	36.8

The normal plots and Pareto charts for the CCD design, presented in Fig. 10, validate the selection of the variables from the fractional factorial design since all four selected variables have a significant effect on the average ΔT . ANOVA was used for average ΔT to evaluate the predicted model by CCD. The results are summarised in Table 7, showing the p-values of the parameters and the coefficient of prediction (R-squared predicted), which is higher than 90%.

Table 7. CCD model ANOVA results for ΔT

Model	P-value					Model		
	Mould Temperature	Cooling time	Holding time	Barrel Temperature	Holding time *Barrel Temperature	R-sq %	R-sq(adj)%	R-sq(pred)%
0.000	0.000	0.000	0.004	0.000	0.007	95.43	94.51	92.24

4.3 Optimisation by using the desirability function and RSM model

The design optimiser in Minitab 20 was applied to use the desirability function, and the result for ΔT is illustrated in Fig. 10. Based on this result, the optimum process setting to minimise the ΔT , at a value of just under 5.1 °C, is summarised in Table 8. The desirability value for this single response is equal to 1 based on equations (8) to (10).



Fig. 10. Optimisation by desirability function for single response ΔT

Table 8. Optimum process settings found by desirability function for ΔT

Mould Temperature (°C)	Cooling time (s)	Holding time (s)	Barrel Temperature (°C)	Avg ΔT (°C)
90	30	7.5	195	5.1

After single-response optimisation, a multi-objective optimisation was performed using the desirability function in Minitab 20. The result for the optimum process settings to provide a process with the minimum cycle time and ΔT is summarised in Table 9 and Fig. 11. Based on this result, using the optimum settings in Table 9, ΔT will be 7.42 °C and the cycle time 30.28 s. The individual desirability value for ΔT ($d_1(y_1)$) is equal to 0.72102 and for cycle time ($d_2(y_2)$) is 0.82617. So, the composite desirability based on equation 8 with n=2 will be 0.7718. The weight (w) of each response was considered 1 in equation 9.

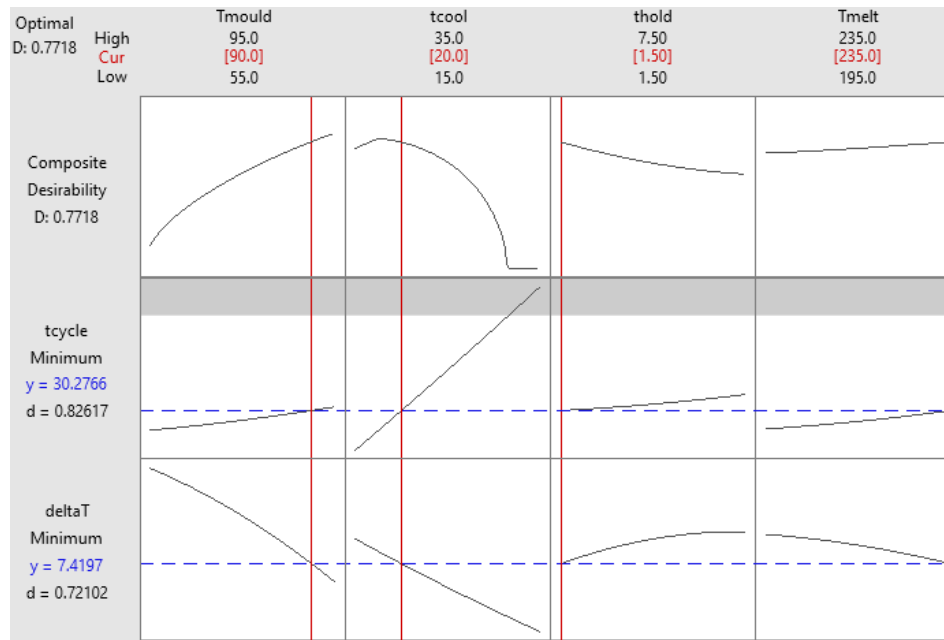


Fig. 11. Optimisation by desirability function for multi-response ΔT and cycle time

Table 9. Optimum process settings found by desirability function for multi-response optimisation

Mould Temperature (°C)	Cooling time (s)	Holding time (s)	Barrel Temperature (°C)	Avg ΔT (°C)	Cycle time (s)
90	20	1.5	235	7.42	30.28

4.4 ADoE

For the comparison of the adaptive DoE in finding the optimum settings with CCD, the same testing strategy was applied. The ADoE was first carried out for the ΔT and then for the ΔT and cycle time as the multi-objective optimisation approach.

The twelve experiments were randomly selected from CCD as prior data for the Bayesian optimisation, and the optimisation process was followed based on the flowchart in Fig. 6. The optimum setting was found for the ΔT after just four more experiments (or two loops in the flowchart), and the experimental settings converged based on the stopping criterion outlined in section 3.3 for single response optimisation. The extra four experiments are listed in Table 10. A total of 16 experiments were required to find the optimum setting for the single optimisation of ΔT .

Table 10. Optimum process settings found by ADoE for average ΔT after four experiments

No	Mould Temperature (°C)	Cooling time (s)	Holding time (s)	Barrel Temperature (°C)	ΔT (°C)
13	90.5	30	7.2	195	5.85
14	93.95	30	6.8	195	5.84
15	90	30	7.5	195.5	5.54
16	90	30	7.5	195.5	5.54

For the multi-objective ADoE, a similar approach was followed based on Fig. 6. After conducting ten more experiments using the Bayesian optimisation approach (5 loops of the flowchart) in addition to the initial 12 experiments, a desired value for the ΔT and cycle time were found, 6.51°C and 32.9s respectively (Table 11) on the stopping criterion mentioned in section 3.3 for multi-response optimisation. For the multi-objective design, a total of 22 experiments were conducted, which is more efficient than the initial CCD experiments with 31 designs.

Table 11. Optimum process settings found by ADoE for average ΔT and cycle time after ten experiments

No.	Mould Temperature (°C)	Cooling time (s)	Holding time (s)	Barrel Temperature (°C)	ΔT (°C)	Cycle time (s)
1	90	30	2.3	195	6.3	39.6
2	88.6	24.8	4.5	200.7	6.96	36.6
3	90	30	7.5	195.5	5.54	44.8
4	70	20.2	2.35	231.5	10.19	29.8
5	87.1	24.8	1.92	199.5	7.21	34.02

6	90	28.3	1.75	195.2	6.75	37.35
7	90	30	4.5	195.3	6.16	41.1
8	90	25	1.5	195	6.8	33.8
9	90	20	1.5	195	7.77	28.8
10	90	24.1	1.5	195.1	6.51	32.9

4.5 NSGA-II

The RSM models for ΔT and cycle time were derived utilising CCD data. These models were then employed as objective functions in the NSGA-II approach to determine the optimal process settings aimed at minimising both ΔT and cycle time. The lower and upper bounds of input parameters were defined in Table 6. Thirty-five optimal Pareto fronts were found by NSGA-II and are indicated in Fig.12. Based on this figure, a higher ΔT will result in a longer cycle time, as expected.

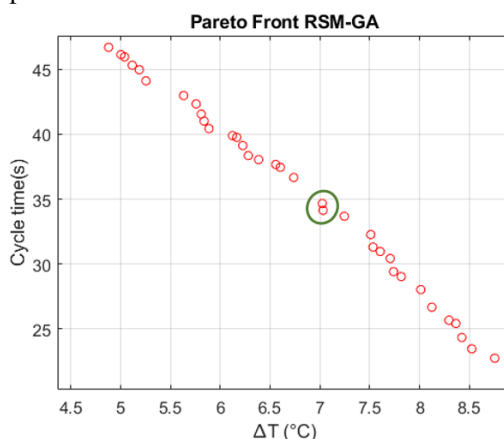


Fig. 12. Pareto fronts of NSGA-II optimisation approach to minimise cycle time and ΔT

Based on the desired threshold defined for the responses, $\Delta T \leq 7^\circ\text{C}$ and cycle time $\leq 33\text{s}$, there are only two appropriate solutions as shown with a green circle in the figure. Between these two solutions, the one with a lower cycle time is desirable. Table 12 summarises the input parameters and responses for this selected Pareto optimal solution. This solution resulted in a cycle time of 34.14s and ΔT of 7.03s.

Table 12. NSGA-II optimal Pareto front

Mould Temperature ($^\circ\text{C}$)	Cooling time (s)	Holding time (s)	Barrel Temperature ($^\circ\text{C}$)	Predicted ΔT ($^\circ\text{C}$)	Predicted Cycle time (s)
88.30	1.63	26.24	198.48	34.14	7.03

4.6 Comparison of optimisation with ADoE approach, desirability function and NSGA-II

The result of each method is summarised in Table 13. CCD requires a further additional experiment to test the predicted optimum values, while ADoE is based on the experimental results when convergence to the desired performance is known to be achieved. Both the predicted and actual responses for the CCD are outlined in the table. The first advantage of ADoE over the other two optimisation approaches, presented in Table 13, is that it uses significantly fewer experiments for optimisation. The number of experiments for the single optimisation of ΔT was almost halved, from 31 experiments for CCD to 16 for ADoE. For the multi-response optimisation, the number of experiments for ADoE was reduced to 22 compared to 31 for the desirability function and NSGA-II. The predicted optimum process settings for the single optimisation of ΔT applying desirability function and ADoE are similar, as indicated in Table 13. Since ADoE results are based on the experimental data, a good agreement between the experimental results ($\Delta T = 5.54^\circ\text{C}$) and optimisation using the desirability function ($\Delta T = 5.10^\circ\text{C}$) can be observed. The predicted optimum process settings for multi-response optimisation using the desirability function for CCD were also conducted in experiments for verification. The experimental values for ΔT and cycle time were 8.2°C , and 28.8s, and the estimated values by desirability function based on Table 13 were 7.42°C and 30.28s. The errors in cycle time and ΔT prediction for CCD were almost 5% and 10%, respectively

From Table 13, it is also evident that for the optimisation of the ΔT , both methods found similar process settings. However, for the multi-optimisation of the cycle time and ΔT , the barrel temperature is 235°C for the desirability function and 195.1°C for ADoE. The temperature of 235°C is relatively high for the POM material and causes other defects in the part, such as burn marks. The ADoE framework with a Gaussian process trained on 12 initial experiments was successful after four experiments (repeating the flowchart of Fig. 6 twice) and determined that for optimising the ΔT and cycle time together, the barrel temperature should stay around 195°C .

The NSGA-II optimal process settings closely mirror those for ADoE optimal settings in multiobjective optimisation, differing mainly in a longer cooling time of approximately 2 seconds. The average RMSE values, approximately 1s and 0.21°C for cycle time and ΔT , suggest that this predicted optimal setting aligns closely with the experimental one obtained through ADoE. However, it took a total number of 31 experiments to build the RSM models and apply the optimisation algorithm for NSGA-II, along with one additional experiment for validation. In contrast, ADOE required only 22 experiments to identify the optimal responses. Furthermore, the ADoE-based yielded a smaller ΔT and a shorter cycle time, both of which are more desirable outcomes.

Table 13. Optimum process parameters found by CCD and ADoE for ΔT and cycle time

Optimisation Method	No of Experiments	Mould Temperature (°C)	Cooling time (s)	Holding time (s)	Barrel temperature (°C)	ΔT (°C)		Cycle time (s)	
						Predicted	Actual	Predicted	Actual
Single desirability function	31	90	30	7.5	195	5.10	5.54	-	-
Single ADoE	16	90	30	7.5	195.5	-	5.54	-	-
multi-desirability function	31	90	20	1.5	235	7.42	8.2	30.28	28.8
multi ADoE	22	90	24.1	1.5	195.1	-	6.51	-	32.9
NSGA-II	31	89	26	1.63	198.5	7.04	6.83	34.14	34.93

The correlation between dimensional stability and ΔT is clear in Table 5 and Fig. 8. The height (H) is always within the defined tolerance boundary for any ΔT value, but the tolerances for length (L) and width (W) decrease considerably as ΔT decreases. For example, a reduction in ΔT from 10.19°C to 5.54°C corresponds to a significant decrease in tolerance error for the length of the component (L), from 150.4% (-0.3mm) to 46.6% (-0.093mm). The optimum process settings found by ADoE resulted in parts meeting the dimensional tolerances. ΔT values below 7.5°C resulted in components satisfying the dimensional tolerance requirement. However small increases in ΔT above this threshold corresponded in one or more dimensions being out of tolerance and therefore a lower target range of ΔT from 6.5°C to 7°C is recommended to ensure the resulting components will meet specification. In the future, more data on the relationship between ΔT and the dimensional stability of the parts could help to tune the optimum threshold more exactly, to ensure required part quality without extending the cooling time any longer than necessary.

One further point to mention is that the initial dataset for the ADoE method included data from twelve randomly selected CCD runs. Using a smaller or different baseline dataset can affect the ADoE loop in Fig. 6, making it longer or shorter depending on the selected data. However, irrespective of the starting dataset, the ADoE approach can be expected to converge on the same optimum process settings for minimising the cycle time and temperature differential. In this research, the optimisation process for CCD and ADoE was done in less than two days by conducting more than sixty experiments. In contrast, even with a high-spec system, running the sixty simulations is significantly time-consuming and typically requires several days as well as expertise with expensive simulation software.

5. Conclusion

In this research, a Bayesian adaptive design of experiment method (ADoE) was used in an experimental IM process to optimise product quality and cycle time. In ADoE the real-time response of the component must be assessed rapidly, so the desired outputs included the cycle time, which was recorded from the machine, and in-line temperature differential (ΔT), which could be calculated quickly using data collected from the two thermocouples. In this proposed approach for prediction of the product quality by ADoE and using ΔT , only one simulation was conducted in Moldflow to identify the hotspot locations and place the sensors. The inline ΔT was used a predictor of dimensional stability and shrinkage verified by metrology. A classic DOE approach, full central composite design (CCD), combined with desirability function and NSGA-II algorithm was also implemented for comparison to ADoE. Injection moulding experiments were conducted on an industrial-standard machine to verify and compare the methods using the same moulded component. The ADoE approach improves significantly on the standard other approaches in both single and multi-objective optimisation, in terms of efficiency (no of experiments) and the performance of the resulting recommended settings.

The Bayesian adaptive design applies prior knowledge to iterate toward the optimum process settings. Also, since the Bayesian adaptive DoE implements both exploitation (where the objective mean is high) and exploration (where the uncertainty is high) for searching, it requires a smaller dataset, offering better performance than CCD. This study implemented ADoE in an actual injection moulding machine and validated the efficiency of ADOE in an actual manufacturing process using experimental and inline data rather than simulation data (Gao & Wang, 2009; Jung et al., 2022). Not only is the experimental approach more reliable, it is also faster than running an

equivalent number of simulations. It has the further advantage that it can be quickly adapted on changing raw material batch or other changes to machine set-up.

ADoE requires a smaller dataset compared to the classic DoE methods that are used for optimisation of injection moulding processes. Since running experiments can be expensive, resource-intensive, and time-consuming, ADoE can reduce the optimisation cost, scrap rates, and enhance the overall component quality by decreasing defects associated with warpage and shrinkage. The proposed approach was applied for two responses; however, the approach could be extended to consider other responses such as energy or material consumption. Future studies can compare this type of ADoE to other adaptive DoE approaches using different starting set of experiments, surrogate models, or acquisition functions and also include a larger range of responses.

Acknowledgement

This publication has emanated from research supported by an ATU Sligo Bursary and a grant from Science Foundation Ireland under Grant number 16/RC/3872. For the purpose of Open Access, the author has applied a CC BY public copyright licence to any Author Accepted Manuscript version arising from this submission.

Statements and Declarations

The authors declare no conflict of interests.

References

- Anand, F. S., Lee, J. H., & Realf, M. J. (2010). Optimal decision-oriented Bayesian design of experiments. *Journal of Process Control*, 20(9), 1084–1091. <https://doi.org/10.1016/j.jprocont.2010.06.011>
- Bischi, B., Richter, J., Bossek, J., Horn, D., Thomas, J., & Lang, M. (2017). *mlrMBO: A Modular Framework for Model-Based Optimization of Expensive Black-Box Functions*. <http://arxiv.org/abs/1703.03373>
- Box, G. E. P., & Draper, N. R. (1987). Empirical model-building and response surfaces. In *Empirical model-building and response surfaces*. John Wiley & Sons.
- Castellano-Quero, M., Castillo-López, M., Fernández-Madrigal, J. A., Arévalo-Espejo, V., Voos, H., & García-Cerezo, A. (2023). A multidimensional Bayesian architecture for real-time anomaly detection and recovery in mobile robot sensory systems. *Engineering Applications of Artificial Intelligence*, 125(January), 106673. <https://doi.org/10.1016/j.engappai.2023.106673>
- Cho, S., Kim, M., Lee, J., Han, A., Na, J., & Moon, I. (2023). Multi-objective optimization of explosive waste treatment process considering environment via Bayesian active learning. *Engineering Applications of Artificial Intelligence*, 117(September 2022), 105463. <https://doi.org/10.1016/j.engappai.2022.105463>
- Deb, K. (2011). Multi-objective Optimisation Using Evolutionary Algorithms: An Introduction. In L. Wang, A. H. C. Ng, & K. Deb (Eds.), *Multi-objective Evolutionary Optimisation for Product Design and Manufacturing* (pp. 3–34). Springer London. https://doi.org/10.1007/978-0-85729-652-8_1
- Deb, K., Pratap, A., Agarwal, S., & Meyarivan, T. (2002). A fast and elitist multiobjective genetic algorithm: NSGA-II. *IEEE Transactions on Evolutionary Computation*, 6(2), 182–197. <https://doi.org/10.1109/4235.996017>
- Derringer, G., & Suich, R. (1980). Simultaneous Optimization of Several Response Variables. *Journal of Quality Technology*, 12(4), 214–219. <https://doi.org/10.1080/00224065.1980.11980968>
- Fang, M., Zhu, Z., & Zhang, Z. (2022). Numerical simulation of closed plastic impeller molding process and its parameter optimization. *Scientific Reports*, 12(1), 17335. <https://doi.org/10.1038/s41598-022-22260-7>
- Feng, Q. Q., Liu, L., & Zhou, X. (2020). Automated multi-objective optimization for thin-walled plastic products using Taguchi, ANOVA, and hybrid ANN-MOGA. *International Journal of Advanced Manufacturing Technology*, 106(1–2), 559–575. <https://doi.org/10.1007/s00170-019-04488-2>
- Frazier, P. I. (2018). *A Tutorial on Bayesian Optimization. Section 5*, 1–22. <http://arxiv.org/abs/1807.02811>
- Gao, Y., & Wang, X. (2009). Surrogate-based process optimization for reducing warpage in injection molding. *Journal of Materials Processing Technology*, 209(3), 1302–1309. <https://doi.org/10.1016/j.jmatprotec.2008.03.048>
- Greenhill, S., Rana, S., Gupta, S., Vellanki, P., & Venkatesh, S. (2020). Bayesian Optimization for Adaptive

- Experimental Design: A Review. *IEEE Access*, 8, 13937–13948. <https://doi.org/10.1109/ACCESS.2020.2966228>
- Hoffer, J. G., Ranftl, S., & Geiger, B. C. (2023). Robust Bayesian target value optimization. *Computers & Industrial Engineering*, 180(May), 109279. <https://doi.org/10.1016/j.cie.2023.109279>
- Imani, M., & Ghoreishi, S. F. (2020). Bayesian Optimization Objective-Based Experimental Design. *Proceedings of the American Control Conference, 2020-July*, 3405–3411. <https://doi.org/10.23919/ACC45564.2020.9147824>
- Jung, J., Park, K., Cho, B., Park, J., & Ryu, S. (2022). Optimization of injection molding process using multi-objective bayesian optimization and constrained generative inverse design networks. *Journal of Intelligent Manufacturing*. <https://doi.org/10.1007/s10845-022-02018-8>
- Kariminejad, M., Kadivar, M., McAfee, M., McGranaghan, G., & Tormey, D. (2022). Comparison of Conventional and Conformal Cooling Channels in the Production of a Commercial Injection-Moulded Component. *Key Engineering Materials*, 926, 1821–1831. <https://doi.org/10.4028/p-q2k0v8>
- Kim, J. Y., Garcia, D., Zhu, Y., Higdon, D. M., & Yu, H. Z. (2022). A Bayesian learning framework for fast prediction and uncertainty quantification of additively manufactured multi-material components. *Journal of Materials Processing Technology*, 303(February), 117528. <https://doi.org/10.1016/j.jmatprotec.2022.117528>
- Kumar, V., & Kumar, D. (2021). A Systematic Review on Firefly Algorithm: Past, Present, and Future. *Archives of Computational Methods in Engineering*, 28(4), 3269–3291. <https://doi.org/10.1007/s11831-020-09498-y>
- Lee, D. H., Jeong, I. J., & Kim, K. J. (2018). A desirability function method for optimizing mean and variability of multiple responses using a posterior preference articulation approach. *Quality and Reliability Engineering International*, 34(3), 360–376. <https://doi.org/10.1002/qre.2258>
- Li, K., Yan, S., Zhong, Y., Pan, W., & Zhao, G. (2019). Multi-objective optimization of the fiber-reinforced composite injection molding process using Taguchi method, RSM, and NSGA-II. *Simulation Modelling Practice and Theory*, 91(July 2018), 69–82. <https://doi.org/10.1016/j.simpat.2018.09.003>
- Liu, T.-W., Bai, J.-B., Fantuzzi, N., Bu, G.-Y., & Li, D. (2022). Multi-objective optimisation designs for thin-walled deployable composite hinges using surrogate models and Genetic Algorithms. *Composite Structures*, 280(July 2021), 114757. <https://doi.org/10.1016/j.compstruct.2021.114757>
- Lu, Y., & Huang, H. (2020). Multi-objective Optimization of Injection Process Parameters Based on EBFNN and NSGA-II. *Journal of Physics: Conference Series*, 1637(1), 012117. <https://doi.org/10.1088/1742-6596/1637/1/012117>
- Luh, Y. P., Wang, H. L., Iao, H. W., & Kuo, T. C. (2019). Using hotspot analysis to establish non-equidistant cooling channels automatically. *Journal of the Chinese Institute of Engineers, Transactions of the Chinese Institute of Engineers, Series A*, 42(8), 690–699. <https://doi.org/10.1080/02533839.2019.1660226>
- Moayyedean, M., & Mamedov, A. (2019). Multi-objective optimization of injection molding process for determination of feasible moldability index. *Procedia CIRP*, 84(March), 769–773. <https://doi.org/10.1016/j.procir.2019.04.213>
- Močkus, J. (1975). On bayesian methods for seeking the extremum. In *Optimization Techniques IFIP Technical Conference Novosibirsk, July 1–7, 1974* (pp. 400–404). Springer Berlin Heidelberg. https://doi.org/10.1007/3-540-07165-2_55
- Mondal, S., Gwynn, D., Ray, A., & Basak, A. (2020). Investigation of melt pool geometry control in additive manufacturing using hybrid modeling. *Metals*, 10(5), 1–23. <https://doi.org/10.3390/met10050683>
- Mukras, S. M. S. (2020). Experimental-based optimization of injection molding process parameters for short product cycle time. *Advances in Polymer Technology*, 2020. <https://doi.org/10.1155/2020/1309209>
- Mukras, S. M. S., Omar, H. M., & Al-Mufadi, F. A. (2019). Experimental-Based Multi-objective Optimization of Injection Molding Process Parameters. *Arabian Journal for Science and Engineering*, 44(9), 7653–7665. <https://doi.org/10.1007/s13369-019-03855-1>

- Nguyen, H.-T., Nguyen, M.-Q., Manh, N. Q., & Vu, N.-C. (2022). *Numerical Simulation and Multi-objective Optimization of Injection Molding Parameters for Improving the Quality of Plastic Product* (B. T. Long, H. S. Kim, K. Ishizaki, N. D. Toan, I. A. Parinov, & Y.-H. Kim (eds.); pp. 199–205). Springer International Publishing. https://doi.org/10.1007/978-3-030-99666-6_31
- Oh, S. H., Ha, J. W., & Park, K. (2022). Adaptive Conformal Cooling of Injection Molds Using Additively Manufactured TPMS Structures. *Polymers*, *14*(1). <https://doi.org/10.3390/polym14010181>
- Öktem, H., & Shinde, D. (2021). Determination of Optimal Process Parameters for Plastic Injection Molding of Polymer Materials Using Multi-Objective Optimization. *Journal of Materials Engineering and Performance*, *30*(11), 8616–8632. <https://doi.org/10.1007/s11665-021-06029-z>
- Pandita, P., Tsilifis, P., Awalgaonkar, N. M., Bilonis, I., & Panchal, J. (2021). Surrogate-based sequential Bayesian experimental design using non-stationary Gaussian Processes. *Computer Methods in Applied Mechanics and Engineering*, *385*, 114007. <https://doi.org/10.1016/j.cma.2021.114007>
- Pareek, C. M., Tewari, V. K., & Machavaram, R. (2023). Multi-objective optimization of seeding performance of a pneumatic precision seed metering device using integrated ANN-MOPSO approach. *Engineering Applications of Artificial Intelligence*, *117*(October 2022), 105559. <https://doi.org/10.1016/j.engappai.2022.105559>
- Ranade, S. S., & Thiagarajan, P. (2017). Selection of a design for response surface. *IOP Conference Series: Materials Science and Engineering*, *263*(2). <https://doi.org/10.1088/1757-899X/263/2/022043>
- Roslan, N., Rahim, S. Z. A., Abdellah, A. E. H., Abdullah, M. M. A. B., Błoch, K., Pietrusiewicz, P., Nabiałek, M., Szmidla, J., Kwiatkowski, D., Vasco, J. O. C., Saad, M. N. M., & Ghazali, M. F. (2021). Optimisation of shrinkage and strength on thick plate part using recycled ldpe materials. *Materials*, *14*(7). <https://doi.org/10.3390/ma14071795>
- Shahriari, B., Swersky, K., Wang, Z., Adams, R. P., & De Freitas, N. (2016). Taking the human out of the loop: A review of Bayesian optimization. *Proceedings of the IEEE*, *104*(1), 148–175. <https://doi.org/10.1109/JPROC.2015.2494218>
- Sharpe, C., Seepersad, C. C., Watts, S., & Tortorelli, D. (2018). *Design of Mechanical Metamaterials via Constrained Bayesian Optimization. Volume 2A*: <https://doi.org/10.1115/DETC2018-85270>
- Singh, G., Pradhan, M. K., & Verma, A. (2018). Multi Response optimization of injection moulding Process parameters to reduce cycle time and warpage. *Materials Today: Proceedings*, *5*(2), 8398–8405. <https://doi.org/10.1016/j.matpr.2017.11.534>
- Sudsawat, S., & Sriseubsai, W. (2018). Warpage reduction through optimized process parameters and annealed process of injection-molded plastic parts. *Journal of Mechanical Science and Technology*, *32*(10), 4787–4799. <https://doi.org/10.1007/s12206-018-0926-x>
- Sun, J., Tang, Y., Wang, J., Wang, X., Wang, J., Yu, Z., Cheng, Q., & Wang, Y. (2022). A multi-objective optimisation approach for activity excitation of waste glass mortar. *Journal of Materials Research and Technology*, *17*, 2280–2304. <https://doi.org/10.1016/j.jmrt.2022.01.066>
- Toh, H. T., & Hassan, A. (2021). *Quality Improvement in a Multi-cavity Injection Moulding Process Using Response Surface Methodology BT - Proceedings of the 2nd International Conference on Experimental and Computational Mechanics in Engineering: ICECME 2020, Banda Aceh, October 13–14* (Akhyar (ed.); pp. 277–288). Springer Singapore. https://doi.org/10.1007/978-981-16-0736-3_28
- Usman Jan, Q. M., Habib, T., Noor, S., Abas, M., Azim, S., & Yaseen, Q. M. (2020). Multi response optimization of injection moulding process parameters of polystyrene and polypropylene to minimize surface roughness and shrinkage's using integrated approach of S/N ratio and composite desirability function. *Cogent Engineering*, *7*(1). <https://doi.org/10.1080/23311916.2020.1781424>
- Vahid, A., Rana, S., Gupta, S., Vellanki, P., Venkatesh, S., & Dorin, T. (2018). New Bayesian-Optimization-Based Design of High-Strength 7xxx-Series Alloys from Recycled Aluminum. *JOM*, *70*(11), 2704–2709. <https://doi.org/10.1007/s11837-018-2984-z>
- Wen, T., Chen, X., Yang, C., Liu, L., & Hao, L. (2014). Optimization of processing parameters for minimizing warpage of large thin-walled parts in whole stages of injection molding. *Chinese Journal of Polymer Science*, *32*(11), 1535–1543. <https://doi.org/10.1007/s10118-014-1541-7>

- Wu, W., He, X., Li, B., & Shan, Z. (2022). An Effective Shrinkage Control Method for Tooth Profile Accuracy Improvement of Micro-Injection-Molded Small-Module Plastic Gears. *Polymers*, *14*(15), 3114. <https://doi.org/10.3390/polym14153114>
- Xia, W., Luo, B., & Liao, X. P. (2011). An enhanced optimization approach based on Gaussian process surrogate model for process control in injection molding. *International Journal of Advanced Manufacturing Technology*, *56*(9–12), 929–942. <https://doi.org/10.1007/s00170-011-3227-4>
- Xue, D., Balachandran, P. V., Hogden, J., Theiler, J., Xue, D., & Lookman, T. (2016). Accelerated search for materials with targeted properties by adaptive design. *Nature Communications*, *7*, 1–9. <https://doi.org/10.1038/ncomms11241>
- Xue, T., Wallin, T. J., Menguc, Y., Adriaenssens, S., & Chiaramonte, M. (2020). Machine learning generative models for automatic design of multi-material 3D printed composite solids. *Extreme Mechanics Letters*, *41*, 100992. <https://doi.org/10.1016/j.eml.2020.100992>
- Yang, S., Chen, H., Feng, Z., Qin, Y., Zhang, J., Cao, Y., & Liu, Y. (2023). Intelligent multiobjective optimization for high-performance concrete mix proportion design: A hybrid machine learning approach. *Engineering Applications of Artificial Intelligence*, *126*, 106868. <https://doi.org/10.1016/j.engappai.2023.106868>
- Zhang, Z., & Jiang, B. (2007). Optimal process design of shrinkage and sink marks in injection molding. *Journal of Wuhan University of Technology-Mater. Sci. Ed.*, *22*(3), 404–407. <https://doi.org/10.1007/s11595-006-3404-8>
- Zhao, P., Zhang, J., Dong, Z., Huang, J., Zhou, H., Fu, J., & Turng, L.-S. (2020). Intelligent Injection Molding on Sensing, Optimization, and Control. *Advances in Polymer Technology*, *2020*, 1–22. <https://doi.org/10.1155/2020/7023616>
- Zhijun, Y., Wang, H., Wei, X., Yan, K., & Gao, C. (2019). Multiobjective optimization method for polymer injection molding based on a genetic algorithm. *Advances in Polymer Technology*, *2019*. <https://doi.org/10.1155/2019/9012085>
- Zhou, J., & Turng, L. S. (2007). Process optimization of injection molding using an adaptive surrogate model with Gaussian process approach. *Polymer Engineering and Science*, *47*(5), 684–694. <https://doi.org/10.1002/pen.20741>